


Article

Error-Tracking Iterative Learning Control for the Constrained Flexible-Joint Manipulator with Initial Errors

Huihui Shi  and Qiang Chen *

Data-Driven Intelligent Systems Laboratory, College of Information Engineering, Zhejiang University of Technology, Hangzhou 310023, China

* Correspondence: sdnjchq@zjut.edu.cn

Abstract: The use of manipulators can improve sustainable energy utilization efficiency and increase sustainable manufacturing practices for solar tracking systems and manufactures, and thus it is significant to guarantee a high tracking accuracy for manipulators. In this paper, an error-tracking adaptive iterative learning control (AILC) method is proposed for a constrained flexible-joint manipulator (FJM) with initial errors. Due to the existence of the repeated positioning drift, the accuracy of the actual manipulator and the sustainable energy utilization efficiency are affected, which motivates the error-tracking approach proposed in this paper to deal with the repeat positioning problem. The desired error trajectory is constructed, such that the tracking error can follow the desired error trajectory without arbitrary initial values and iteration-varying tasks. Then, the system uncertainties are approximated by the capability of fuzzy logic systems (FLSs), and the combined adaptive laws are designed to update the weight and the approximating error of FLSs. Considering the safety operation of the flexible-joint manipulator, both input and output constraints are considered, a quadratic-fractional barrier Lyapunov function (QFBLF) is constructed, such that the system output is always within the constrained region. Therefore, the proposed method can guarantee the output tracking accuracy of manipulators under arbitrary initial values and iteration-varying tasks and keep the system output within the constraints to improve the transient performance, such that the energy utilization and accessory manufacturing efficiency can be improved. Through the Lyapunov synthesis, it is proved that the tracking error can converge to zero as the number of iterations goes to infinity. Finally, comparative simulations are carried out to verify the effectiveness of the proposed method.

Keywords: flexible-joint manipulator; constraints; error-tracking AILC; fuzzy logic systems; barrier Lyapunov function; sustainable energy utilization efficiency



Citation: Shi, H.; Chen, Q. Error-Tracking Iterative Learning Control for the Constrained Flexible-Joint Manipulator with Initial Errors. *Sustainability* **2022**, *14*, 12453. <https://doi.org/10.3390/su141912453>

Academic Editors: Xiaqing Bai, Chun Wei, Peijie Li and Dongliang Xiao

Received: 9 August 2022

Accepted: 23 September 2022

Published: 30 September 2022

Publisher's Note: MDPI stays neutral with regard to jurisdictional claims in published maps and institutional affiliations.



Copyright: © 2022 by the authors. Licensee MDPI, Basel, Switzerland. This article is an open access article distributed under the terms and conditions of the Creative Commons Attribution (CC BY) license (<https://creativecommons.org/licenses/by/4.0/>).

1. Introduction

With the acceleration of industrialization, the social demand for energy is also increasing rapidly. Renewable energy systems using sustainable energy have attracted extensive attention and utilization. In order to improve the efficiency and use of renewable energy system, industrial manipulators and unmanned aerial vehicles have been widely applied [1–5]; for example, a solar photovoltaic system uses the manipulator to realize the real-time tracking of solar energy, the development of intelligent charging manipulator is also extremely important to solve the problem of “difficult charging” of new energy vehicles, and so on. The flexible-joint manipulator has a series of advantages, such as being lightweight, having a low energy consumption, and a high flexibility, and the FJMs have favorable physical compliance and safety [6–9]. Therefore, in the industrial production including renewable energy systems, the FJMs are in great demand. However, the flexible-joint manipulator is an underactuated system with strong coupling and unknown uncertainties [9], and the existence of the joint elasticity causes the oscillation, which brings challenges in the control design of the flexible-joint manipulator that cannot be neglected. As is known, manipulators have been widely applied in many sustainable manufacturing

and sustainable energy systems to ensure products' economic characteristics, maintain safety, and reduce energy and resource consumption [10–12]; for instance, sustainable manufacturing robots [12], solar panel cleaning robots [13], solar tracking robots [14], and so forth. ABB's (Asea Brown Boveri) robots help Absolicon stably produce solar panels, improve the capacity of the new energy industry, and play a key role in global sustainable technology. A large-workspace two-DOF parallel robot for solar tracking systems was proposed in [14] for solar tracking systems, where the manipulators could follow the sun's apparent motion during the year. A U-2PUS parallel robot was presented in [15], as an efficient solar tracking system that could operate at different latitudes. With the development of the equipment and the requirement for a high energy utilization, higher requirements are put forward for tracking accuracy of the manipulators. Consequently, it is significant to design a manipulator controller to guarantee the high tracking accuracy of manipulators.

To this day, various control methods have been presented for the tracking problem of the flexible-joint manipulator, such as adaptive control, robust control, sliding mode control, iterative learning control, and so on [16–18]. Due to the repeatability of the operation tasks of the FJM, the contraction-mapping-based iterative learning control (ILC) method improves the tracking performance gradually by utilizing the previous information of the control input and error [19–21]. Different from the ILC methods based on the contraction mapping theory, the adaptive iterative learning control (AILC) method is a parametric learning method based on the Lyapunov theorem, which contains the advantages of both the ILC and the adaptive control methods, and the AILC method can indirectly improve the control performance by updating the estimation of the unknown control parameters [22–26]. One of the essential assumptions of the ILC and AILC methods is the identical initial condition. In fact, the identical initial condition can be hardly satisfied due to the limitation of the system repeatability in practical industrial operations. To relax the restriction on the initial condition, two main techniques containing a boundary layer method and an initial rectifying method were proposed based on the ILC and AILC methods [27–29]. The initial rectifying method rectified the original reference trajectory by constructing a smooth transition trajectory, such that the identical initial condition was achieved artificially, and the arbitrary initial state value was allowed. As an alternative, the error-tracking approach proposed in [30] could guarantee the actual output error tracked the desired error reference trajectory perfectly over a period of time. In our previous works [31,32], it could be seen that the desired error trajectory was independent of the original reference trajectory, such that the controller design would be carried out with ease with the iteration-varying tasks. Another essential assumption of the ILC and AILC methods is the iteration-invariant tasks. In fact, due to the unpredictable factors in the practical industrial operations, the tasks are always iteration-varying [33]. The iteration-varying tasks make the previous learning information become invalid, and the system needs to restart the learning process for even a small change of the tasks. In order to address the iteration-varying tasks, some effective works have been developed on the ILC and AILC design [34–36]. However, the aforementioned results on the AILC methods cannot directly be applied in the constrained flexible-joint manipulator under arbitrary initial values and iteration-varying tasks.

It should be noted that constraints commonly exist in industrial operations, such as input saturation, hysteresis, friction, and so on, which may result in a system performance degradation and even instability [37–41]. To compensate for the effect of unknown input constraints, many advanced approximation tools including fuzzy logic systems and neural networks have been utilized in the controller design [42,43]. Meanwhile, the output constraint has also attracted attention since when the output of the system violates the limitation of the system, the system tracking performance is affected and even unstable. In order to handle the output constraint, barrier Lyapunov functions (BLFs) including Tan-type BLF and log-type BLF were proposed [44–47], so that the violation of the system output constraints could be avoided. In [46], an adaptive fuzzy fault-tolerant control for switched systems was proposed based on a log-type BLF, the unmeasurable states were handled by a switched state observer, and the system output satisfied the constrained interval. The

proposed universal BLF in [47] could effectively deal with the output constraints and could work greatly in both constrained and unconstrained situations. Moreover, the flexible-joint manipulator was constrained by the limitation of the torque input, and the end-effector should be constrained for the safety of the operation [48–50]. Therefore, it is significant to take the input and output constraints into account in the controller design.

Inspired by the aforementioned discussions, an error-tracking adaptive learning control method is proposed for a constrained flexible-joint manipulator with initial errors. The restrictions on the initial value and the operation tasks are relaxed by the proposed method, and the accessory manufacturing, and energy utilization efficiency are improved. The uncertainties of the flexible-joint manipulator are approximated by FLSs. For the operation safety of the flexible-joint manipulator, the input and output constraints are considered, and with the constructed quadratic-fractional barrier Lyapunov function, the constraint is not violated within the finite time interval. The main contributions are summarized as follows.

(i) The error-tracking adaptive learning control method is proposed for a constrained flexible-joint manipulator with initial errors, which can solve the output tracking problem under arbitrary initial values and iteration-varying tasks. The system uncertainties are approximated by FLSs, and the combined adaptive laws are designed to update the weights of the FLSs.

(ii) For the safety operation of the constrained flexible-joint manipulator, the quadratic-fractional barrier Lyapunov function is constructed, such that the system output is always within the constraints. The tracking error is guaranteed to converge to zero as the number of iterations goes to infinity by a rigorous stability analysis.

The rest of this article is organized as follows. The transformation of the flexible-joint manipulator and some preliminaries are shown in Section 2. In Section 3, the error-tracking adaptive learning control and the combined adaptive law are designed, and the quadratic-fractional barrier Lyapunov function is constructed for the safety operation. A stability analysis of the constrained flexible-joint manipulator is given in Section 4. In Section 5, the comparative simulations are shown, and the superiority of the proposed method is verified. A significant conclusion is drawn in Section 6.

2. Problem Formulation

2.1. System Description and Transformation

Considering a constrained flexible-joint manipulator performing iteration-varying tasks, shown in Figure 1, the dynamic model of the constrained FJM [6] is described by

$$\begin{aligned} I\ddot{q}_{1,k} + K(q_{1,k} - q_{2,k}) + MgL \sin(q_{1,k}) &= 0 \\ J\ddot{q}_{2,k} - K(q_{1,k} - q_{2,k}) &= \text{sat}(u_k) \end{aligned} \quad (1)$$

where $q_{1,k}$ and $q_{2,k}$ are the angles of the link and motor at the k th iteration, respectively; I and J are the inertia of the link and motor, respectively; K is the spring stiffness; g is the gravity term; M is the link mass; L is the length between the center of gravity the flexible joint; and $\text{sat}(u_k)$ is the control torque with the input saturation at the k th iteration.

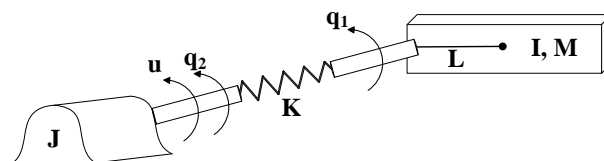


Figure 1. The model of a single-link flexible-joint manipulator.

Let $x_{1,k} = q_{1,k}$, $x_{2,k} = \dot{q}_{1,k}$, $x_{3,k} = q_{2,k}$, $x_{4,k} = \dot{q}_{2,k}$. The system (1) can be rewritten as

$$\begin{cases} \dot{x}_{1,k} = x_{2,k} \\ \dot{x}_{2,k} = -\frac{K}{I}(x_{1,k} - x_{3,k}) - \frac{MgL}{I} \sin(x_{1,k}) \\ \dot{x}_{3,k} = x_{4,k} \\ \dot{x}_{4,k} = \frac{K}{J}(x_{1,k} - x_{3,k}) + \frac{1}{J} \text{sat}(u_k) \end{cases} \quad (2)$$

The input saturation is expressed as

$$\text{sat}(u_k) = \begin{cases} u_{\max}, & u_k \geq u_{\max} \\ u_k, & u_{\min} \leq u_k \leq u_{\max} \\ u_{\min}, & u_k \leq u_{\min} \end{cases} \quad (3)$$

where $u_{\max} > 0$ and $u_{\min} < 0$ are the maximum and minimum values of the control input, respectively.

The saturation is compensated by the hyperbolic function in the form of

$$r(u_k) = u_{\max} \times \tanh\left(\frac{u_k}{u_{\max}}\right) = u_{\max} \frac{e^{\frac{u_k}{u_{\max}}} - e^{-\frac{u_k}{u_{\max}}}}{e^{\frac{u_k}{u_{\max}}} + e^{-\frac{u_k}{u_{\max}}}} \quad (4)$$

Then, the input saturation can be rewritten as

$$\text{sat}(u_k) = r(u_k) + \Delta u_k \quad (5)$$

where $\Delta u_k = \text{sat}(u_k) - r(u_k)$ is a bounded estimating error, which satisfies $|\Delta u_k| = |\text{sat}(u_k) - r(u_k)| \leq u_{\max}(1 - \tanh(1)) = D_s'$.

Through the mean-value theorem, one has

$$r(u_k) = r(u_0) + r_{u_\varrho}(u_k - u_0) \quad (6)$$

where $u_\varrho = \varrho u_k + (1 - \varrho)u_0$, $u_0 \in [0, u_k]$, and $\varrho \in (0, 1)$ is a positive constant. $r_{u_\varrho} = \frac{\partial r(u_k)}{\partial u_k} |_{u_k = u_\varrho}$, and $r_{u_\varrho} \in (0, 1]$.

By choosing $u_0 = 0$, (6) can be rewritten as

$$r(u_k) = r_{u_\varrho} u_k \quad (7)$$

Taking (7) into (5) yields

$$\text{sat}(u_k) = r_{u_\varrho} u_k + \Delta u_k \quad (8)$$

Then, substituting (8) into (2) leads to

$$\begin{cases} \dot{x}_{1,k} = x_{2,k} \\ \dot{x}_{2,k} = -\frac{K}{I}(x_{1,k} - x_{3,k}) - \frac{MgL}{I} \sin(x_{1,k}) \\ \dot{x}_{3,k} = x_{4,k} \\ \dot{x}_{4,k} = \frac{K}{J}(x_{1,k} - x_{3,k}) + \frac{1}{J} r_{u_\varrho} u_k + \frac{1}{J} \Delta u_k \end{cases} \quad (9)$$

The nonlinear state coordinate transformation is defined as

$$\begin{cases} z_{1,k} = x_{1,k} \\ z_{2,k} = x_{2,k} \\ z_{3,k} = -\frac{K}{I}(x_{1,k} - x_{3,k}) - \frac{MgL}{I} \sin(x_{1,k}) \\ z_{4,k} = -\frac{K}{I}(x_{2,k} - x_{4,k}) - \frac{MgL}{I} x_{2,k} \cos(x_{1,k}) \end{cases} \quad (10)$$

Therefore, by the transformation (10), the flexible-joint manipulator (9) can be transformed into

$$\begin{cases} \dot{z}_{1,k} = z_{2,k} \\ \dot{z}_{2,k} = z_{3,k} \\ \dot{z}_{3,k} = z_{4,k} \\ \dot{z}_{4,k} = f(\bar{z}_k) + bu_k + \frac{K}{IJ} \Delta u_k \end{cases} \quad (11)$$

where $f(\bar{z}_k) = \frac{MgL}{I} \sin(z_{1,k})(z_{2,k}^2 - \frac{K}{J}) - (\frac{MgL}{I} \cos(z_{1,k}) + \frac{K}{J} + \frac{K}{I})z_{3,k}$, $\bar{z}_k = [z_{1,k}, z_{2,k}, z_{3,k}]^T$, $f(\bar{z}_k)$ is abbreviated for f_k , and $b = \frac{K}{IJ} r_{u_q}$ is an unknown gain constant. From $|\Delta u_k| \leq D_s < 0$, $r_{u_q} \in (0, 1]$, and K, I, J are unknown positive constants, one has $\frac{K}{IJ} |\Delta u_k| \leq D_s < 0$, and $b > 0$ is an unknown bounded constant. It is assumed that there exists a positive constant b_{\min} , such that $0 < b_{\min} \leq b$.

The output tracking error and the state errors are defined as

$$\begin{aligned} e_{1,k} &= z_{1,k} - y_{d,k}, & e_{2,k} &= z_{2,k} - \dot{y}_{d,k} \\ e_{3,k} &= z_{3,k} - \ddot{y}_{d,k}, & e_{4,k} &= z_{4,k} - y_{d,k}^{(3)} \end{aligned} \quad (12)$$

where $y_{d,k}$ is the iteration-varying reference trajectory, which is continuous and fourth-order differentiable.

From (11) and (12), the error dynamic of the flexible-joint manipulator is obtained as

$$\begin{cases} \dot{e}_{1,k} = e_{2,k} \\ \dot{e}_{2,k} = e_{3,k} \\ \dot{e}_{3,k} = e_{4,k} \\ \dot{e}_{4,k} = f_k + bu_k + \frac{K}{IJ} \Delta u_k - y_{d,k}^{(4)} \end{cases} \quad (13)$$

2.2. Construction of the Desired Error Trajectory

Adaptive iterative learning control (AILC) is an effective control method to achieve high accuracy when operating repetitive tasks. However, there is the practical problem of repeated positioning drift, which affects the accuracy of the actual manipulator and even affects the sustainable energy utilization efficiency. Identical initial condition is a common restriction to solve the repeated positioning drift in the learning process of the traditional ILC and AILC design [19],

$$\begin{aligned} z_{1,k}(0) &= y_{d,k}(0), z_{2,k}(0) = \dot{y}_{d,k}(0) \\ z_{3,k}(0) &= \ddot{y}_{d,k}(0), z_{4,k}(0) = y_{d,k}^{(3)}(0) \end{aligned} \quad (14)$$

However, due to the limitation of repositioning accuracy and unpredictable factors in the operation of the flexible-joint manipulator, the restriction is hardly satisfied. In order to relax the repeated setting of the initial value in the flexible-joint manipulator operation, initial rectifying methods, time-varying boundary layer methods, and some other methods have been proposed [27–29]. Different from those various methods, the

error-tracking iterative learning control approach proposed in this section effectively deals with the initial state problem by constructing a smooth fourth-order desired error trajectory for the flexible-joint manipulator performing iteration-varying tasks (11), and the amount of calculation is decreased, since there is no need to reconstruct the desired error trajectory.

The construction conditions of the desired error trajectory $e_{r,k}(t)$ are given as follows,

$$e_{r,k}(0) = e_{1,k}(0), e_{r,k}^{(m)}(0) = \frac{1}{m!} e_{1,k}^{(m)}(0), e_{r,k}^{(4)}(0) = 0, \quad (15)$$

$$e_{r,k}^{(i)}(T_s) = 0, \quad (16)$$

where $e_{r,k}(0)$ and $e_{r,k}^{(m)}(0)$ are the initial values of the desired error trajectory and its derivatives, $e_{1,k}(0)$ and $e_{1,k}^{(m)}(0)$ are the initial values of the output error and state errors of the flexible-joint manipulator, $e_{r,k}(T_s)$ and $e_{r,k}^{(i)}(T_s)$ are the values of the desired error trajectory and its derivatives at the access point T_s , where $m = 1, 2, 3$, $i = 0, 1, \dots, 4$.

The fourth-order desired error trajectory is constructed as

$$e_{r,k}(t) = \begin{cases} e_{\zeta,k}(t), & t \in [0, T_s] \\ 0, & t \in (T_s, T] \end{cases} \quad (17)$$

Remark 1. The desired error trajectory is constructed by a transition trajectory $e_{\zeta,k}(t)$ and a trajectory with a value of zero. In order to relax the initial restriction, the condition (15) is needed to keep the same initial values of $e_{r,k}(0)$ and $e_{1,k}(0)$, $e_{r,k}^{(m)}(0)$ and $e_{1,k}^{(m)}(0)$, respectively. Moreover, the condition (16) is important to keep the desired error trajectory smooth and differentiable at the access point $t = T_s$. Furthermore, the construction conditions do not restrict the initial state and error values, and $e_{1,k}(0)$ can be arbitrary bounded value.

The transition trajectory is designed as

$$e_{\zeta,k}(t) = \sum_{\sigma=0}^9 \gamma_{\sigma} t^{\sigma} \quad (18)$$

in which,

$$\gamma_0 = e_{1,k}(0), \gamma_1 = \dot{e}_{1,k}(0), \gamma_2 = \frac{1}{2} \ddot{e}_{1,k}(0), \gamma_3 = \frac{1}{6} e_{1,k}^{(3)}(0), \gamma_4 = 0,$$

$$\gamma_5 = -\frac{1}{T_s^5} (15\gamma_3 T_s^3 + 35\gamma_2 T_s^2 + 70\gamma_1 T_s + 126\gamma_0),$$

$$\gamma_6 = \frac{1}{T_s^6} (40\gamma_3 T_s^3 + 105\gamma_2 T_s^2 + 224\gamma_1 T_s + 420\gamma_0),$$

$$\gamma_7 = -\frac{1}{T_s^7} (45\gamma_3 T_s^3 + 126\gamma_2 T_s^2 + 280\gamma_1 T_s + 540\gamma_0),$$

$$\gamma_8 = \frac{1}{T_s^8} (24\gamma_3 T_s^3 + 70\gamma_2 T_s^2 + 160\gamma_1 T_s + 315\gamma_0),$$

$$\gamma_9 = -\frac{1}{T_s^9} (5\gamma_3 T_s^3 + 15\gamma_2 T_s^2 + 35\gamma_1 T_s + 70\gamma_0),$$

and $e_{1,k}(0)$, $\dot{e}_{1,k}(0)$, $\ddot{e}_{1,k}(0)$, $e_{1,k}^{(3)}(0)$ are the initial values of the output tracking error and its differentiations. T_s is the access point, and T is the time interval at each iteration.

Remark 2. The transition trajectory coefficients $\gamma_\sigma, \sigma = 0, 1, \dots, 9$ are calculated based on the construction conditions (15) and (16),

$$\begin{aligned} \gamma_0 &= e_{1,k}(0), \gamma_1 = \dot{e}_{1,k}(0), \gamma_2 = \frac{1}{2!}\ddot{e}_{1,k}(0), \gamma_3 = \frac{1}{3!}e_{1,k}^{(3)}(0), \gamma_4 = 0, \\ \sum_{\sigma=0}^9 \gamma_\sigma T_s^\sigma &= 0, \sum_{\sigma=1}^9 \sigma \gamma_\sigma T_s^{\sigma-1} = 0, \sum_{\sigma=2}^9 \sigma(\sigma-1)\gamma_\sigma T_s^{\sigma-2} = 0, \\ \sum_{\sigma=3}^9 \sigma(\sigma-1)(\sigma-2)\gamma_\sigma T_s^{\sigma-3} &= 0, \sum_{\sigma=3}^9 \sigma(\sigma-1)(\sigma-2)(\sigma-3)\gamma_\sigma T_s^{\sigma-4} = 0 \end{aligned}$$

such that the desired error trajectory is smooth and differentiable, and the initial state and error values can be arbitrary bounded values.

The control objective is to design an error-tracking adaptive iterative learning controller for a flexible-joint manipulator (1) with input saturation (3) under the constraints, such that the output tracking error $e_{1,k}$ can completely track the desired error trajectory during $t \in [0, T]$ as the number of iterations goes to infinity; in other words, the system output $x_{1,k}$ can completely track the iteration-varying reference trajectory $y_{d,k}$ during $t \in [T_s, T]$.

2.3. Fuzzy Logic Systems

Typical fuzzy logic systems are composed of four basic parts: the knowledge base, the fuzzy inference engine, the fuzzifier, and the defuzzifier [43]. The knowledge base is formed from fuzzy inference rules, i.e., “IF-THEN” rules:

R^l : If x_1 is F_1^l and x_2 is F_2^l and \dots and x_n is F_n^l , then y is $G^l, l = 1, \dots, N$. where $x = [x_1, \dots, x_n]^T \in R^n$ and $y \in R$ are the input and output of the fuzzy logic system, respectively, F_i^l and G^l are the fuzzy set, and N is the number of fuzzy inference rules. The fuzzy membership functions of F_i^l and G^l are given as $\mu_{F_i^l}(x_i)$ and $\mu_{G^l}(y), i = 1, \dots, N$, respectively.

Then, by applying the singleton fuzzifier, the product inference, and the center average defuzzification, the output of the FLS can be written as

$$y(x) = \frac{\sum_{l=1}^N \vartheta_l \prod_{i=1}^n \mu_{F_i^l}(x_i)}{\sum_{l=1}^N \left[\prod_{i=1}^n \mu_{F_i^l}(x_i) \right]} \tag{19}$$

where $\vartheta_l = \max_{y \in R} \mu_{G^l}(y), l = 1, \dots, N$.

The fuzzy basis function is defined as

$$\varphi_l(x) = \frac{\prod_{i=1}^n \mu_{F_i^l}(x_i)}{\sum_{l=1}^N \left[\prod_{i=1}^n \mu_{F_i^l}(x_i) \right]}, l = 1, \dots, N. \tag{20}$$

Denote $\phi(X) = [\varphi_1(x), \dots, \varphi_N(x)]^T, \theta^T = [\vartheta_1, \dots, \vartheta_N]^T$; then, the FLS can be described as

$$y(x) = \theta^T \phi(X). \tag{21}$$

Lemma 1 ([51]). Suppose that the input universe of discourse Ω is a compact set in R^n . Then, for any given real continuous function $h(x)$ on Ω and arbitrary $\delta^* > 0$, there exists an FLS (21) and an optimal parameter vector θ^* such that

$$\sup_{x \in \Omega} |h(x) - \theta^{*T} \phi(X)| \leq \delta^* \tag{22}$$

3. Error-Tracking Iterative Learning Control Design

In this section, an error-tracking iterative learning controller is designed for the constrained flexible-joint manipulator (11) with initial errors based on the constructed error-

tracking trajectory (17), such that the output tracking error $e_{1,k}$ can track the desired error trajectory during $t \in [0, T]$ as the number of iterations goes to infinity, and the high accuracy and fast tracking of the FJM can be achieved to improve accessory manufacturing, and sustainable energy utilization efficiency. The following Lemma is introduced for the controller design.

Lemma 2 ([52]). *If the derivative of the sequence $z_k(t)$ is uniformly bounded on $[0, T]$, and*

$$\lim_{k \rightarrow \infty} \int_0^T z_k^2(t) dt = 0, t \in [0, T] \quad (23)$$

then, $\lim_{k \rightarrow \infty} e_k(t) = 0$ uniformly on $[0, T]$.

Define $\varepsilon_{i,k}$, $i = 1, \dots, 4$ as

$$\begin{cases} \varepsilon_{1,k} = e_{1,k} - e_{r,k} \\ \varepsilon_{2,k} = e_{2,k} - \dot{e}_{r,k} \\ \varepsilon_{3,k} = e_{3,k} - \ddot{e}_{r,k} \\ \varepsilon_{4,k} = e_{4,k} - e_{r,k}^{(3)} \end{cases} \quad (24)$$

and define z_k as

$$z_k = \lambda_1 \varepsilon_{1,k} + \lambda_2 \varepsilon_{2,k} + \lambda_3 \varepsilon_{3,k} + \varepsilon_{4,k} \quad (25)$$

where $\lambda_j, j = 1, \dots, 3$ is selected such that $P(D) = D^3 + \lambda_3 D^2 + \lambda_2 D + \lambda_1$ is a Hurwitz polynomial, and it is clear that $z_k(0) = 0$ from the definition of the desired error trajectory.

Differentiating z_k results in

$$\begin{aligned} \dot{z}_k &= \lambda_1 \varepsilon_{2,k} + \lambda_2 \varepsilon_{3,k} + \lambda_3 \varepsilon_{4,k} + \dot{\varepsilon}_{4,k} \\ &= \varepsilon_k + f_k + bu_k + \frac{K}{IJ} \Delta u_k \end{aligned} \quad (26)$$

where $\varepsilon_k = \lambda_1 \varepsilon_{2,k} + \lambda_2 \varepsilon_{3,k} + \lambda_3 \varepsilon_{4,k} - y_{d,k}^{(4)} - e_{r,k}^{(4)}$.

Choose the quadratic-fractional barrier Lyapunov function as

$$V_{1,k}(t) = \frac{1}{2b} \frac{z_k^2}{k_c^2 - \varepsilon_{1,k}^2} \quad (27)$$

where k_c is a positive constant, which is the constraint of $\varepsilon_{1,k}$.

Differentiating (27) yields

$$\begin{aligned} \dot{V}_{1,k}(t) &= \frac{z_k}{b(k_c^2 - \varepsilon_{1,k}^2)} \dot{z}_k + \frac{z_k^2 \varepsilon_{1,k} \varepsilon_{2,k}}{b(k_c^2 - \varepsilon_{1,k}^2)^2} \\ &= \frac{z_k \rho_k}{b} \dot{z}_k + \frac{z_k^2 \rho_k^2 \varepsilon_{1,k} \varepsilon_{2,k}}{b} \end{aligned} \quad (28)$$

where $\rho_k = (k_c^2 - \varepsilon_{1,k}^2)^{-1}$.

Substituting (26) into (28) yields

$$\begin{aligned} \dot{V}_{1,k}(t) &= \frac{z_k \rho_k}{b} (\varepsilon_k + f_k + bu_k + \frac{K}{IJ} \Delta u_k) + \frac{z_k^2 \rho_k^2 \varepsilon_{1,k} \varepsilon_{2,k}}{b} \\ &= z_k \rho_k \left(u_k + \frac{K \Delta u_k}{IJb} + \frac{\varepsilon_k + f_k}{b} + \frac{z_k \rho_k \varepsilon_{1,k} \varepsilon_{2,k}}{b} \right) \\ &= z_k \rho_k \left(u_k + \bar{f}_k + \frac{K \Delta u_k}{IJb} \right) \end{aligned} \quad (29)$$

where $\bar{f}_k = \frac{1}{b}(e_k + f_k + 2\rho_k z_k \varepsilon_{1,k} \varepsilon_{2,k})$.

Using the approximation tool fuzzy logic system, the unknown function \bar{f}_k can be approximated as

$$\bar{f}_k = \theta^{*T} \phi_k + \delta_k \quad (30)$$

where $\theta^* \in R^N$ is the ideal weight of the fuzzy logic system, ϕ_k is the active function, and δ_k is the approximating error, which satisfies $|\delta_k| \leq \delta_N$.

Taking (30) into (29) leads to

$$\begin{aligned} \dot{V}_{1,k}(t) &= z_k \rho_k \left(u_k + \theta^* \phi_k + \delta_k + \frac{K\Delta u_k}{I J b} \right) \\ &\leq z_k \rho_k (u_k + \theta^* \phi_k) + |z_k \rho_k| \left| \delta_k + \frac{K\Delta u_k}{I J b} \right| \\ &\leq z_k \rho_k (u_k + \theta^* \phi_k) + |z_k \rho_k| \delta_D \end{aligned} \quad (31)$$

where δ_D is a positive constant and $\delta_D = \delta_N + \frac{D_s}{b_{\min}} \geq |\delta_k + \frac{K\Delta u_k}{I J b}|$.

Choose the positive Lyapunov function $V_k(t)$ as

$$V_k(t) = V_{1,k}(t) + V_{2,k}(t) = V_{1,k}(t) + \frac{1-\zeta}{2\eta} \tilde{\theta}_k^T \tilde{\theta}_k + \frac{1-\alpha}{2\beta} \tilde{\delta}_k^2 \quad (32)$$

where $\tilde{\theta}_k = \theta^* - \hat{\theta}_k$ and $\tilde{\delta}_k = \delta_D - \hat{\delta}_k$ are the estimation error of θ^* and δ_D , respectively, and $\hat{\theta}_k$ and $\hat{\delta}_k$ are the estimation of δ_D , respectively. $\zeta, \eta, \alpha, \beta$ are all positive constants.

Differentiating (32) yields

$$\begin{aligned} \dot{V}_k(t) &= \dot{V}_{1,k}(t) + \frac{1-\zeta}{\eta} \tilde{\theta}_k^T \dot{\tilde{\theta}}_k + \frac{1-\alpha}{\beta} \tilde{\delta}_k \dot{\tilde{\delta}}_k \\ &\leq z_k \rho_k (u_k + \theta^* \phi_k) + |z_k \rho_k| \delta_D + \frac{1-\zeta}{\eta} \tilde{\theta}_k^T \dot{\tilde{\theta}}_k + \frac{1-\alpha}{\beta} \tilde{\delta}_k \dot{\tilde{\delta}}_k \end{aligned} \quad (33)$$

Design the adaptive iterative learning controller as

$$u_k = -c_1 \rho_k^{-1} z_k - \hat{\delta}_k \text{sign}(z_k \rho_k) - \hat{\theta}_k^T \phi_k \quad (34)$$

where c_1 is a positive constant.

Taking (34) into (33) leads to

$$\begin{aligned} \dot{V}_k(t) &= -c_1 z_k^2 + z_k \rho_k \left(-\hat{\delta}_k \text{sign}(z_k \rho_k) + \tilde{\theta}_k^T \phi_k \right) + |z_k \rho_k| \delta_D + \frac{1-\zeta}{\eta} \tilde{\theta}_k^T \dot{\tilde{\theta}}_k + \frac{1-\alpha}{\beta} \tilde{\delta}_k \dot{\tilde{\delta}}_k \\ &= -c_1 z_k^2 + |z_k \rho_k| \tilde{\delta}_k + z_k \rho_k \tilde{\theta}_k^T \phi_k + \frac{1-\zeta}{\eta} \tilde{\theta}_k^T \dot{\tilde{\theta}}_k + \frac{1-\alpha}{\beta} \tilde{\delta}_k \dot{\tilde{\delta}}_k \end{aligned} \quad (35)$$

The combined adaptive laws are designed to update the $\hat{\theta}_k$ and $\hat{\delta}_k$,

$$(1-\zeta)\dot{\hat{\theta}}_k = -\zeta\hat{\theta}_k + \zeta\hat{\theta}_{k-1} + \eta z_k \rho_k \phi_k \quad (36)$$

$$(1-\alpha)\dot{\hat{\delta}}_k = -\alpha\hat{\delta}_k + \alpha\hat{\delta}_{k-1} + \beta|z_k \rho_k| \quad (37)$$

where $\hat{\theta}_k(0) = \hat{\theta}_{k-1}(T)$, $\hat{\theta}_{-1}(t) = 0$, $\hat{\delta}_k(0) = \hat{\delta}_{k-1}(T)$, and $\hat{\delta}_{-1}(t) = 0$.

4. Convergence Analysis

In this section, the main results are summarized as the theorem below, and the error convergence is proved with the proposed control method.

Theorem 1. For the flexible-joint manipulator (1) with output constraint, by designing the fourth-order desired error trajectory (17), the adaptive iterative learning controller (34), and the combined

adaptive laws (36) and (37), $\lim_{k \rightarrow \infty} z_k(t) = 0$ uniformly on $[0, T]$, the output tracking error $e_{1,k}$ can converge to zero as the number of iterations goes to infinity, and the system output $x_{1,k}$ is guaranteed within the constraint on $[0, T]$.

The Lyapunov-like function is chosen as

$$E_k(t) = V_k(t) + \frac{\zeta}{2\eta} \int_0^t \tilde{\theta}_k^T \tilde{\theta}_k d\tau + \frac{\alpha}{2\beta} \int_0^t \tilde{\delta}_k^2 d\tau \quad (38)$$

The proof process is divided into three parts in the following.

Part I: The boundedness of the $E_k(0)$.

Substituting (36) and (37) into (35) leads to

$$\begin{aligned} \dot{V}_k(t) &\leq -c_1 z_k^2 + |z_k \rho_k| \tilde{\delta}_k + z_k \rho_k \tilde{\theta}_k^T \phi_k - \frac{1-\zeta}{\eta} \tilde{\theta}_k^T \dot{\hat{\theta}}_k - \frac{1-\alpha}{\beta} \tilde{\delta}_k \dot{\hat{\delta}}_k \\ &= -c_1 z_k^2 + |z_k \rho_k| \tilde{\delta}_k + z_k \rho_k \tilde{\theta}_k^T \phi_k + \frac{1}{\eta} \tilde{\theta}_k^T (\zeta \hat{\theta}_k - \zeta \hat{\theta}_{k-1} - \eta z_k \rho_k \phi_k) \\ &\quad + \frac{1}{\beta} \tilde{\delta}_k (\alpha \hat{\delta}_k - \alpha \hat{\delta}_{k-1} - \beta |z_k \rho_k|) \\ &= -c_1 z_k^2 + \frac{\zeta}{\eta} \tilde{\theta}_k^T (\hat{\theta}_k - \hat{\theta}_{k-1}) + \frac{\alpha}{\beta} \tilde{\delta}_k (\hat{\delta}_k - \hat{\delta}_{k-1}) \end{aligned} \quad (39)$$

Differentiating (38) leads to

$$\dot{E}_k(t) = \dot{V}_k(t) + \frac{\zeta}{2\eta} \tilde{\theta}_k^T \dot{\tilde{\theta}}_k + \frac{\alpha}{2\beta} \dot{\tilde{\delta}}_k^2 \quad (40)$$

Substituting (39) into (40) leads to

$$\begin{aligned} \dot{E}_k(t) &\leq -c_1 z_k^2 + \frac{\zeta}{\eta} \tilde{\theta}_k^T (\hat{\theta}_k - \hat{\theta}_{k-1}) + \frac{\alpha}{\beta} \tilde{\delta}_k (\hat{\delta}_k - \hat{\delta}_{k-1}) + \frac{\zeta}{2\eta} \tilde{\theta}_k^T \dot{\tilde{\theta}}_k + \frac{\alpha}{2\beta} \dot{\tilde{\delta}}_k^2 \\ &= -c_1 z_k^2 + \frac{\zeta}{2\eta} \tilde{\theta}_k^T \dot{\tilde{\theta}}_k + \frac{\alpha}{2\beta} \dot{\tilde{\delta}}_k^2 + \frac{\zeta}{2\eta} \left(-(\tilde{\theta}_k - \tilde{\theta}_{k-1})^T (\tilde{\theta}_k - \tilde{\theta}_{k-1}) + \tilde{\theta}_{k-1}^T \tilde{\theta}_{k-1} \right. \\ &\quad \left. - \tilde{\theta}_k^T \tilde{\theta}_k \right) + \frac{\alpha}{2\beta} \left(\tilde{\delta}_{k-1}^2 - \tilde{\delta}_k^2 - (\tilde{\delta}_k - \tilde{\delta}_{k-1})^2 \right) \\ &\leq -c_1 z_k^2 + \frac{\zeta}{2\eta} \tilde{\theta}_{k-1}^T \tilde{\theta}_{k-1} + \frac{\alpha}{2\beta} \tilde{\delta}_{k-1}^2 \end{aligned} \quad (41)$$

When $k = 0$, one has $\tilde{\theta}_{-1} = \theta^*$ and $\tilde{\delta}_{-1} = \delta_D$, and $z_0 = 0$. Then, by integrating both sides of (41), it can be obtained that

$$\begin{aligned} E_0(t) &\leq E_0(0) + \int_0^t \left(\frac{\zeta}{2\eta} \theta^{*T} \theta^* + \frac{\alpha}{2\beta} \delta_D^2 \right) d\tau \\ &= V_0(0) + \int_0^t \left(\frac{\zeta}{2\eta} \theta^{*T} \theta^* + \frac{\alpha}{2\beta} \delta_D^2 \right) d\tau \end{aligned} \quad (42)$$

In (42), $V_0(0)$ is bounded due to the definition of $V_k(t)$ in (27), $z_k(0) = 0$, and $\tilde{\theta}_0(0) = \tilde{\theta}_{-1}(T) = \theta^*$. In addition, $\int_0^t \left(\frac{\zeta}{2\eta} \theta^{*T} \theta^* + \frac{\alpha}{2\beta} \delta_D^2 \right) d\tau$ is bounded in $[0, T]$. Then, it can be obtained that $E_0(t)$ is bounded in $[0, T]$, i.e.,

$$\begin{aligned} E_0(t) &\leq V_0(0) + \left(\frac{\zeta}{2\eta} \theta^{*T} \theta^* + \frac{\alpha}{2\beta} \delta_D^2 \right) T \\ &\leq \infty \end{aligned} \quad (43)$$

Part II: The convergence of z_k .

The difference of $E_k(t)$ between two successive iterations is

$$\begin{aligned} \Delta E_k(t) &= E_k(t) - E_{k-1}(t) \\ &= V_k(0) + \int_0^t \dot{V}_k(\tau) d\tau + \frac{\alpha}{2\beta} \int_0^t (\tilde{\delta}_k^2 - \tilde{\delta}_{k-1}^2) d\tau + \frac{\zeta}{2\eta} \int_0^t (\tilde{\theta}_k^T \tilde{\theta}_k - \tilde{\theta}_{k-1}^T \tilde{\theta}_{k-1}) d\tau - V_{k-1}(t) \\ &\leq V_k(0) - V_{k-1}(t) + \int_0^t \left(-c_1 z_k^2 + \frac{\zeta}{\eta} \tilde{\theta}_k^T (\hat{\theta}_k - \hat{\theta}_{k-1}) + \frac{\alpha}{\beta} \tilde{\delta}_k (\hat{\delta}_k - \hat{\delta}_{k-1}) \right) d\tau \\ &\quad + \frac{\zeta}{2\eta} \int_0^t (\tilde{\theta}_k^T \tilde{\theta}_k - \tilde{\theta}_{k-1}^T \tilde{\theta}_{k-1}) d\tau + \frac{\alpha}{2\beta} \int_0^t (\tilde{\delta}_k^2 - \tilde{\delta}_{k-1}^2) d\tau \end{aligned} \tag{44}$$

With the algebraic condition $(a - b)^2 - (a - c)^2 = 2(a - b)(c - b) - (b - c)^2$, one has

$$\begin{aligned} \Delta E_k(t) &\leq V_k(0) - V_{k-1}(t) + \int_0^t \left(-c_1 z_k^2 + \frac{\zeta}{\eta} \tilde{\theta}_k^T (\hat{\theta}_k - \hat{\theta}_{k-1}) + \frac{\alpha}{\beta} \tilde{\delta}_k (\hat{\delta}_k - \hat{\delta}_{k-1}) \right) d\tau \\ &\quad + \frac{\zeta}{2\eta} \int_0^t \left(2\tilde{\theta}_k^T (\hat{\theta}_{k-1} - \hat{\theta}_k) - (\hat{\theta}_k - \hat{\theta}_{k-1})^T (\hat{\theta}_k - \hat{\theta}_{k-1}) \right) d\tau \\ &\quad + \frac{\alpha}{2\beta} \int_0^t \left(2\tilde{\delta}_k (\hat{\delta}_{k-1} - \hat{\delta}_k) - (\hat{\delta}_k - \hat{\delta}_{k-1})^2 \right) d\tau \\ &\leq V_k(0) - V_{k-1}(t) - \int_0^t c_1 z_k^2 d\tau \end{aligned} \tag{45}$$

When $t = T$, by using the alignment conditions $\hat{\theta}_k(0) = \hat{\theta}_{k-1}(T)$, $\hat{\delta}_k(0) = \hat{\delta}_{k-1}(T)$ and $z_k(0) = 0$, (45) can be rewritten as

$$\begin{aligned} \Delta E_k(T) &\leq -V_{1,k-1}(T) - \int_0^T c_1 z_k^2 d\tau \\ &\leq -\int_0^T c_1 z_k^2 d\tau \end{aligned} \tag{46}$$

It can be concluded that $\Delta E_k(t)$ is negative definite for all iterations. According to the boundedness of $E_0(t)$, the negative definiteness of $\Delta E_k(t)$, and $E_k(T) = E_0(T) + \sum_{k=1}^{\infty} \Delta E_k(T)$, one has the boundedness of $E_k(T)$. It can further be found that there exist finite and positive constants $D_1 > 0$ and $D_2 > 0$, such that

$$\begin{aligned} \frac{\zeta}{2\eta} \int_0^t \tilde{\theta}_k^T \tilde{\theta}_k d\tau + \frac{\alpha}{2\beta} \int_0^t \tilde{\delta}_k^2 d\tau &\leq \frac{\zeta}{2\eta} \int_0^T \tilde{\theta}_k^T \tilde{\theta}_k d\tau + \frac{\alpha}{2\beta} \int_0^T \tilde{\delta}_k^2 d\tau \\ &\leq D_1 < \infty, \quad \forall t \in [0, T]. \end{aligned} \tag{47}$$

$$V_{2,k}(T) = \frac{1 - \zeta}{2\eta} \tilde{\theta}_k^T(T) \tilde{\theta}_k(T) + \frac{1 - \alpha}{2\beta} \tilde{\delta}_k^2(T) \leq D_2 < \infty \tag{48}$$

Substituting (47) into (38) yields

$$\begin{aligned} E_k(t) &= V_k(t) + \frac{\zeta}{2\eta} \int_0^t \tilde{\theta}_k^T \tilde{\theta}_k d\tau + \frac{\alpha}{2\beta} \int_0^t \tilde{\delta}_k^2 d\tau \\ &\leq V_k(t) + D_1 \end{aligned} \tag{49}$$

From (45) and (48), one can obtain

$$\begin{aligned} \Delta E_k(t) &\leq V_k(0) - V_{k-1}(t) - \int_0^t c_1 z_k^2 d\tau \\ &\leq V_{1,k}(0) - V_{1,k-1}(t) + V_{2,k}(0) - V_{2,k-1}(t) \\ &= -V_{1,k-1}(t) + V_{2,k-1}(T) - V_{2,k-1}(t) \\ &\leq D_2 - V_{k-1}(t) \end{aligned} \tag{50}$$

From (49) and (50), one has

$$E_{k+1}(t) = E_k(t) + \Delta E_{k+1}(t) \leq V_k(t) + D_1 + D_2 - V_k(t) = D_1 + D_2 \quad (51)$$

According to (51), the uniform boundedness of $E_k(t)$ is obtained. Thus, $z_k, \varepsilon_{1,k}, \hat{\theta}_k$ and $\hat{\delta}_k$ are uniformly bounded from (38). From (24), (26), and (34), the uniform boundedness of $u_k, e_{i,k}, i = 1, 2, 3, 4, z_k$, and \dot{z}_k can be also obtained.

The finite sum of $\Delta E_k(T)$ is given as

$$\begin{aligned} \sum_{j=1}^k \Delta E_j(T) &= \sum_{j=1}^k (E_j(T) - E_{j-1}(T)) \\ &= E_k(T) - E_0(T) \end{aligned} \quad (52)$$

Substituting (46) into (52) yields

$$\begin{aligned} E_k(T) &= E_0(T) + \sum_{j=1}^k \Delta E_j(T) \\ &\leq E_0(T) - \sum_{j=1}^k \int_0^T c_1 z_j^2 d\tau \\ &= E_0(T) - c_1 \sum_{j=1}^k \int_0^T |z_j|^2 d\tau \end{aligned} \quad (53)$$

For the sake of analysis convenience, (53) can be rewritten as

$$c_1 \sum_{j=1}^k \int_0^T |z_j|^2 d\tau \leq E_0(T) - E_k(T) \quad (54)$$

According to the boundedness of $E_0(T)$ and the positiveness of $E_k(T)$, from (54), one has $\lim_{k \rightarrow \infty} \int_0^T |z_k|^2 d\tau = 0$. Combining with the uniform boundedness of \dot{z}_k , and according to the Lemma 2, one has $\lim_{k \rightarrow \infty} z_k(t) = 0$ uniformly on $[0, T]$.

Remark 3. The sign function in the designed controller (34) and the update law (37) may cause chattering, which will degrade the control performance of the system. In practice, the chattering problem can be effectively solved by replacing the sign function with a hyperbolic tangent function.

Part III: The boundedness of $e_{1,k}$ and $x_{1,k}$.

From the analysis mentioned above, z_k and V_k are bounded, and thus $|\varepsilon_{1,k}| \leq k_c$. In Assumption 1, one has $|y_{d,k}| \leq D_{y_k}$. The desired error trajectory is clearly bounded by $|e_{r,k}| \leq D_e$. From the definition of $\varepsilon_{1,k} = e_{1,k} - e_{r,k} = x_{1,k} - y_{d,k} - e_{r,k}$, both $e_{1,k}$ and $x_{1,k}$ are bounded, and $-k_c + x_{d,k} + e_{r,k} \leq x_{1,k} \leq k_c + x_{d,k} + e_{r,k}$.

5. Simulation

5.1. Numerical Simulation

In this section, comparative illustrations are provided to verify the effectiveness of the proposed error-tracking adaptive iterative learning control method for a constrained flexible-joint manipulator with initial errors (1), and the parameters of system (1) are given as $M = 2$ kg, $L = 1$ m, $K = 10$ N · m/rad, $I = 0.5$ kg · m², $J = 2$ kg · m² and $g = 9.8$ m/s².

The iterations number was set as $KT = 7$, and the iteration-varying trajectory was given as $y_{d,k} = a_k \sin(\omega_k t) + 0.2 \cos(t)$, where $a_k = 0.5 + 0.01 \frac{k}{KT}$, $\omega_k = 1 + 0.01 \frac{k}{KT}$, with k being the current iteration. The initial states in the system (2) were given as $x_{1,k}(0) = 0.5$, $x_{2,k}(0) = -0.02$, $x_{3,k}(0) = 1.45$, $x_{4,k}(0) = -0.05$, $J_k \triangleq \max_{t \in [0, T]} |z_{1,k}(t)|$, and $T = 6$ s. The de-

sired error trajectory was designed in (17), and the access point was set as $T_s = 0.9$ s. For comparison, control methods with or without considering the output constraint are given.

M1: The proposed method with output constraint. The adaptive iterative learning controller of M1 was proposed in (34), and the combined adaptive laws were designed in (36), (37). The parameters were set as: $c_1 = 2$, $\lambda_1 = 1$, $\lambda_2 = 2$, $\lambda_3 = 2$, $\iota = 12$, $\zeta = 0.9$, $\eta = 10$, $\alpha = 0.9$, and $\beta = 2$. The constraint of $\varepsilon_{1,k}$ was given as $k_c = 0.07$, and $\bar{k}_c = k_c + x_{d,k} + e_{r,k}$, $k_c = -k_c + x_{d,k} + e_{r,k}$. The control input was constrained by $u_{\min} = -8$ and $u_{\max} = 20$.

M2: The fuzzy-based AILC method without considering output constraint. When the constraint $k_c \rightarrow \infty$, the constraint requirement was removed, and the following controller was given without considering the output constraint,

$$u_k = -c_1 z_k - \hat{\theta}_k^T \phi_k - \hat{\delta}_k \tanh\left(\frac{z_k}{\iota}\right) \quad (55)$$

and the combined adaptive laws were designed as

$$(1 - \zeta)\hat{\theta}_k = -\zeta\hat{\theta}_k + \zeta\hat{\theta}_{k-1} + \eta z_k \phi_k \quad (56)$$

$$(1 - \alpha)\hat{\delta}_k = -\alpha\hat{\delta}_k + \alpha\hat{\delta}_{k-1} + \beta z_k \tanh\left(\frac{z_k}{\iota}\right) \quad (57)$$

M3: The robust AILC method without considering output constraint. The controller was designed as

$$u_k = -c_1 z_k - \hat{f}_k \text{sgn}(z_k) \quad (58)$$

and the combined adaptive law was designed as

$$(1 - \zeta)\hat{f}_k = -\zeta\hat{f}_k + \zeta\hat{f}_{k-1} + \eta|z_k| \quad (59)$$

where \hat{f}_k is the estimation of f_{\max} , which is the bound of the uncertainties, i.e., $|\bar{f}_k + \frac{K\Delta u_k}{JJb}| \leq f_{\max}$.

The parameters of controllers (55) and (58) of M2 and M3 were given as $c_1 = 5$, $\lambda_1 = 5$, $\lambda_2 = 5$, $\lambda_3 = 2$, and $\iota = 12$, and the parameters of the combined adaptive laws (56) and (57) were set as $\zeta = 0.96$, $\eta = 10, 15, 20$, $\alpha = 0.9$, and $\beta = 2$, respectively. The parameters of the combined adaptive law (59) were given as $\zeta = 0.96$, $\eta = 20$. The control input was constrained by $u_{\min} = -8$ and $u_{\max} = 20$.

In M1 and M2, the fuzzy membership functions were selected as

$$\mu_{F_i^1}(x_i) = \frac{1}{1 + e^{4(x_i+5)}}, \quad (60)$$

$$\mu_{F_i^l}(x_i) = e^{-0.01(x_i+L)^2}, \quad (61)$$

$$\mu_{F_i^{11}}(x_i) = \frac{1}{1 + e^{-6(x_i-5)}} \quad (62)$$

where $L = [4, 3, 2, 1, 0, -1, -2, -3, -4]$, $l = 1, \dots, 9$.

The simulation results are provided with different setting of η in Figures 2–6. In Figure 2, under M1, the angle of the link $x_{1,k}$ is always within the constraint, while under M2 and M3, $x_{1,k}$ violates the constraint at the first iteration. As shown in Figure 3, after seven iterations, the output tracking performance is obtained, the angle of the link $x_{1,k}$ can follow the iteration-varying reference trajectory $y_{d,k}$ under three control methods, and can always remain within the constraint. Figure 4 shows the control input $\psi(u_k)$ with input saturation. In Figure 5, the error tracking performance is given, the output error fast converges to the desired error trajectory, and the tracking error can converge to zero under M1. As can be seen from Figures 2–5, at the first and seventh iterations, the best performance of the system cannot be achieved under M3, while under the M1 and M2 methods, the tracking error can converge to a sufficiently small region. As shown in Figure 5, more iterations are required, such as 100 iterations, so that the tracking error can

converge to a smaller bound under M3; however, it means more storage space is required. The performance indexes of three control methods with different gains are displayed in Figure 6, and compared with M2 and M3, J_k can converge faster and it always remains within the constraint under M1.

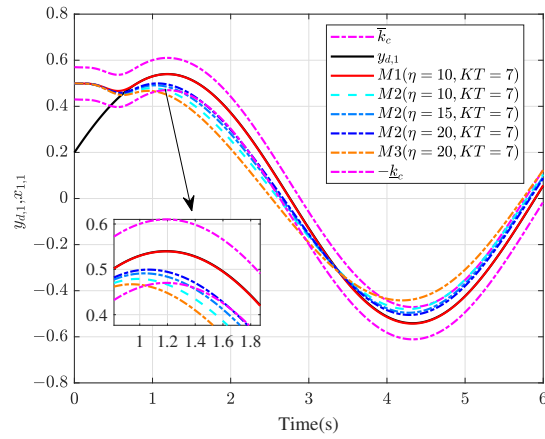


Figure 2. The output tracking performance of system (1) at first iteration.

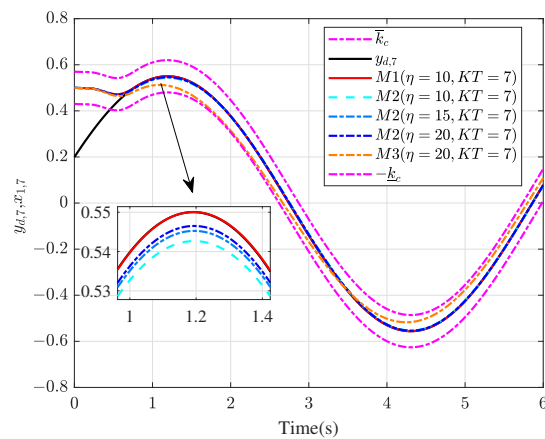


Figure 3. The output tracking performance of system (1) at seventh iteration.

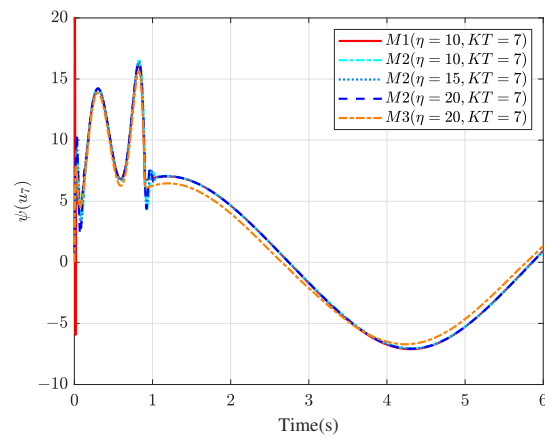


Figure 4. The constrained control input $\psi(u_k)$ at seventh iteration.

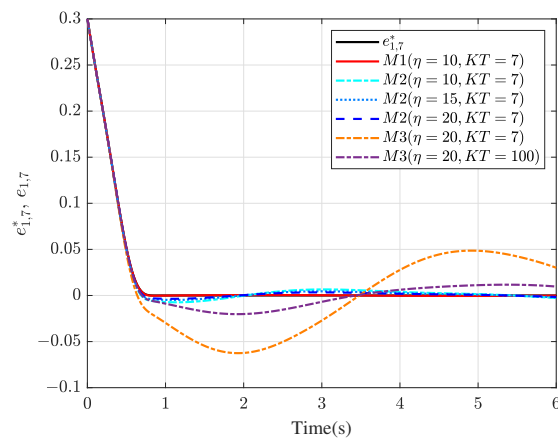


Figure 5. The error tracking performance of system (1) at seventh iteration.

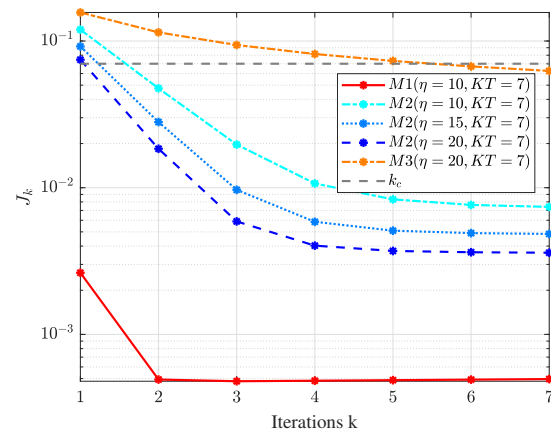


Figure 6. The maximum tracking error J_k of system (1).

To further illustrate the effectiveness of the proposed method, simulation results under different constraints ($k_c = 0.6, k_c = 0.4, k_c = 0.2$, and $k_c = 0.07$) are shown in Figures 7–10. It can be seen from Figure 7 that under different constraints, the proposed M1 method can guarantee that the angle of the link $x_{1,k}$ is always within the constraint range at the first iteration. Figures 8–10 show that after seven iterations, the angle of the link can converge to the iteration-varying trajectory under different constraints, and the smaller the constraint, the better the system output can track the desired trajectory, which means a smaller tracking error can be achieved. From Figure 10, under M1, the performance index J_k convergence is always within the constraint boundary during the iteration process.

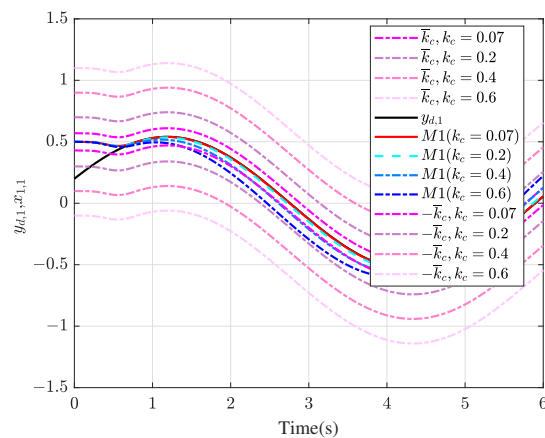


Figure 7. The output tracking performance of system (1) at first iteration with different constraints.

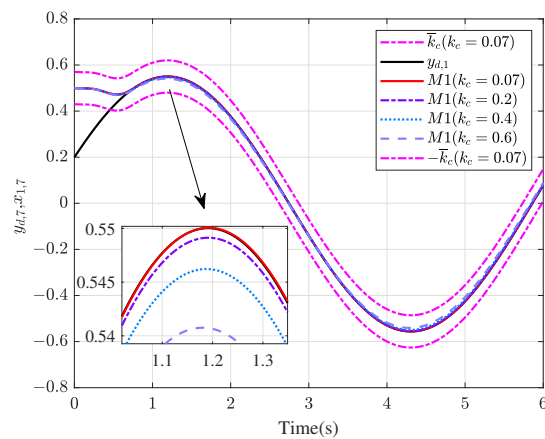


Figure 8. The output tracking performance of system (1) at seventh iteration with different constraints.

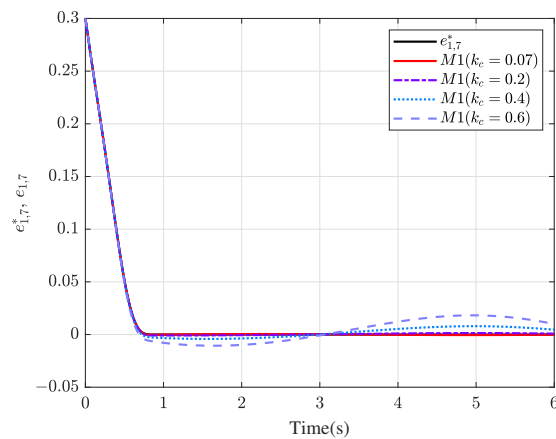


Figure 9. The error tracking performance of system (1) at seventh iteration with different constraints.

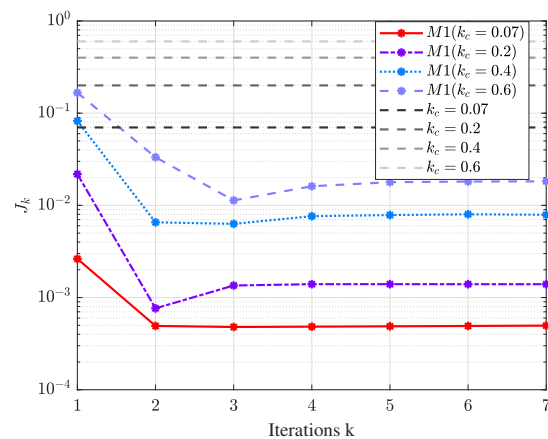


Figure 10. The maximum tracking error J_k of system (1) with different constraints.

In summary, compared with M2 and M3, the tracking error converges to zero faster with lower gain parameters under the proposed M1 method in the interval $t \in [0, T]$. M1 can guarantee the output tracking accuracy of the manipulators under arbitrary initial values and iteration-varying tasks and keep the system output within the constraint to improve the transient performance. Therefore, the proposed AILC scheme is a new way to achieve high sustainable operation.

5.2. Dynamic Simulation

In this section, the block diagram of the trajectory tracking control simulation for the FJM is provided in Figure 11 by using MATLAB Simulink and Solidworks. The dynamic simulation process including the following steps:

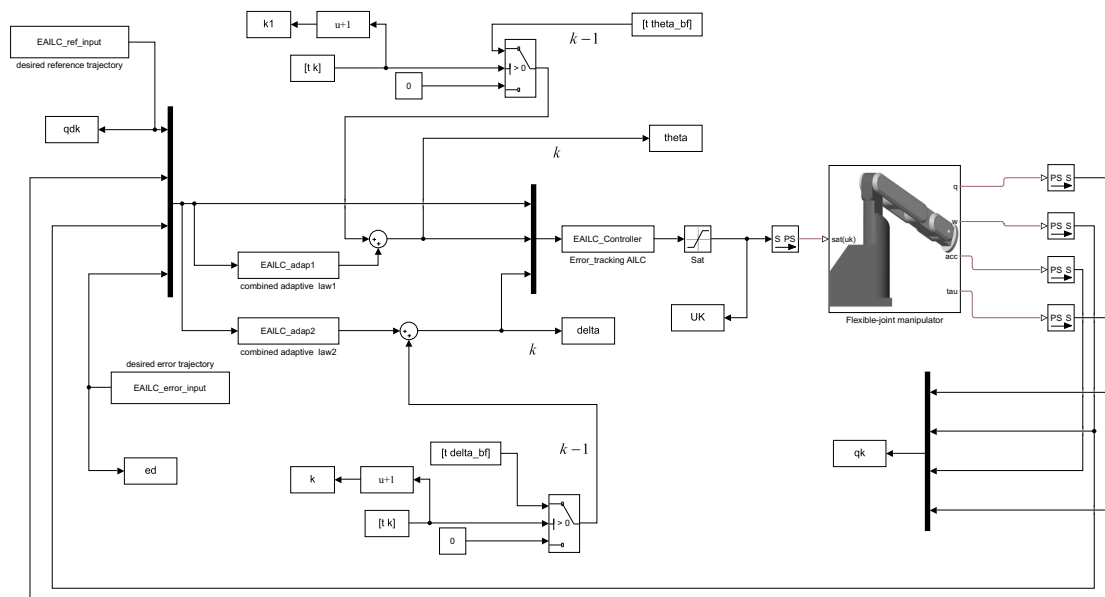


Figure 11. The block diagram of the trajectory tracking control simulation for the FJM.

(1) Use Solidworks and the mechanics toolbox to establish the model of the flexible-joint manipulator (FJM);

(2) Set the basic parameters of the FJM and add the constraints; the mass of the link was 780 kg, the length of the link was 1 m, the spring stiffness was given as $K = 3.27 \text{ N} \cdot \text{m}/\text{rad}$, and the inertia of the link was given as $I = 780 \text{ kg} \cdot \text{m}^2$. The error constraint was given as $k_c = 0.5$. The control input was constrained by $u_{\min} = -10^4$ and $u_{\max} = 10^4$.

(3) Build the simulation model with the MATLAB Simulink to realize the high tracking accuracy for the FJM.

The different sub-blocks are described as follows:

The **Flexible-joint manipulator** block includes the mechanical structure of the FJM, and the system parameters and configuration are given;

The **EAILC_Controller** block presents the proposed error-tracking adaptive iterative learning controller;

The **EAILC_adap1** and **EAILC_adap2** blocks include two combined adaptive laws;

The **[t theta_bf]** and **[t delta_bf]** blocks present two updated variables at the previous iteration;

The **EAILC_ref_input** block includes the reference link angle;

The **EAILC_error_input** block includes the desired error trajectory;

The **qdk**, **ed**, **qk**, **UK**, **theta**, and **delta** blocks are the variables generated by the Simulink environment for each moment from the simulation at the current iteration;

The **sat** block presents a saturation operation.

The iteration number was $K = 12$, and the reference link angle trajectory was $q_{d,k} = 0.5\sin(2t) + 0.1$. The initial link angle and the initial error were $q_{1,k} = 0$ and $e_{1,k} = 0.1$, respectively. $J_k \triangleq \max_{t \in [0, T]} |z_{1,k}(t)|$ and $T = 6 \text{ s}$. The desired error trajectory was designed in (17), and the access point was set as $T_s = 0.3 \text{ s}$. The parameters of the controller were

$c_1 = 20$, $\lambda_1 = 1$, $\lambda_2 = 1$, and $\lambda_3 = 2$, and the parameters of the combined adaptive laws were set as $\zeta = 0.99$, $\eta = 20$, $\alpha = 0.99$, and $\beta = 1800$, respectively. The selection of the fuzzy membership functions was the same as in M1.

Based on the block diagram Figure 11, the trajectory tracking control simulation of the flexible-joint manipulator was provided in a Simulink environment based on the proposed error-tracking adaptive iterative learning controller. The Mechanics Explorer window displays the dynamic simulation, and the generated simulation dynamic process is shown in Figure 12.

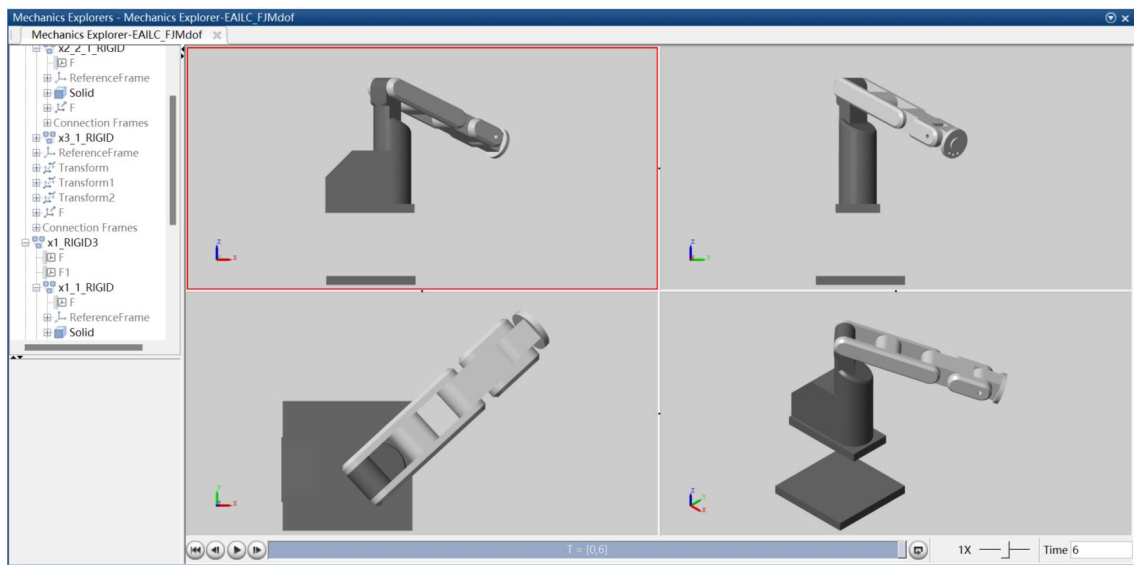


Figure 12. The dynamic simulation of the flexible-joint manipulator.

The main results are shown in Figures 13 and 14. Figure 13 shows the link angle tracking performance for the 1st and 12th iterations, and it can be seen that as the iteration number increases, the link angle gradually follows the reference link angle trajectory with initial errors. Figure 14 displays the performance index; it indicates that the maximum error value decreases with the increase of the iteration number, and a satisfactory tracking performance is achieved. In summary, the results of the simulation demonstrate convincingly that the proposed error-tracking adaptive iterative learning control method is efficient. Moreover, with the increase of the iteration number, the FJM starts to operate repeatedly under the action of the proposed controller and utilizes information in the previous iterations to modify the tracking accuracy and finally track the reference link angle trajectory. Therefore, the proposed AILC method is an effective way to achieve high sustainable operation.

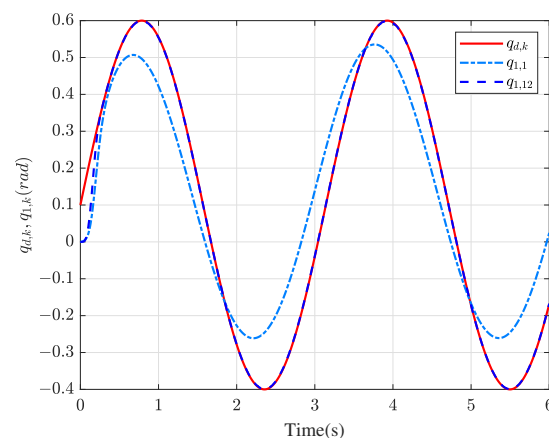


Figure 13. The link angle tracking performance of the FJM at 1st and 12th iteration.

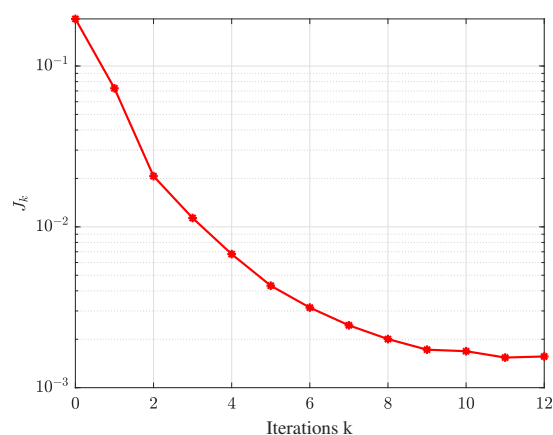


Figure 14. The maximum tracking error J_k of the FJM.

6. Conclusions

For the constrained flexible-joint manipulator with initial errors, an error-tracking adaptive learning control method was proposed, such that the output tracking accuracy of the manipulator was guaranteed under arbitrary initial values and iteration-varying tasks and the sustainable energy utilization efficiency and sustainable manufacturing practices were improved. The quadratic-fractional barrier Lyapunov function could keep the system output within the constraints to improve the transient performance, allowing the FJM to operate safely with iteration-varying tasks. The tracking performance was improved by the FLSs and the combined adaptive laws. Through the error-tracking approach, the repeated positioning problem was solved, such that the proposed method can be appropriate for a real sustainable energy system.

Author Contributions: Conceptualization, Q.C.; methodology, Q.C. and H.S.; validation, H.S.; formal analysis, Q.C. and H.S.; writing—original draft preparation, H.S.; writing—review and editing, Q.C. and H.S. All authors have read and agreed to the published version of the manuscript.

Funding: This research was funded by the National Natural Science Foundation of China (61973274, 62222315, 62233016), the National Natural Science Foundation of Zhejiang Province (LZ22F030007).

Institutional Review Board Statement: Not applicable.

Informed Consent Statement: Not applicable.

Data Availability Statement: Not applicable.

Conflicts of Interest: The authors declare no conflict of interest. The funders had no role in the design of the study; in the collection, analyses, or interpretation of data; in the writing of the manuscript; or in the decision to publish the results.

References

1. Fan, D.; Dong, B.; Wang, S.; Zhao, L.; Wan, L.; Xu, Z.; Wu, Y. Research process of self-cleaning technologies on solar panels. *Mater. Rev.* **2015**, *29*, 111–115. [\[CrossRef\]](#)
2. Wang, T.; Zhang, T.; Liang, J.; Chen, J. Design and field test of a rover robot for antarctic based on renewable energy. *J. Mech. Eng.* **2013**, *49*, 21–30. [\[CrossRef\]](#)
3. Wei, C.; Zhao, Y.; Zheng, Y.; Xie, L.; Smedley, K.M. Analysis and design of a nonisolated high step-down converter with coupled inductor and ZVS operation. *IEEE Trans. Ind. Electron.* **2022**, *69*, 9007–9018. [\[CrossRef\]](#)
4. Tao, M.; Chen, Q.; He, X.; Xie, S. Fixed-time filtered adaptive parameter estimation and attitude control for quadrotor UAVs. *IEEE Trans. Aerosp. Electron. Syst.* **2022**, *ahead of print*. [\[CrossRef\]](#)
5. Feng, C.; Liang, B.; Li, Z.; Liu, W.; Wen, F. Peer-to-peer energy trading under network constraints based on generalized fast dual ascent. *IEEE Trans. Smart Grid* **2022**, *ahead of print*. [\[CrossRef\]](#)
6. Spong, M.; Vidyasagar, M. *Robot Dynamics and Control*; Wiley: New York, NY, USA, 1989.
7. Jin, M.; Lee, J.; Tsagarakis, N.G. Model-free robust adaptive control of humanoid robots with flexible joints. *IEEE Trans. Ind. Electron.* **2017**, *64*, 1706–1715. [\[CrossRef\]](#)

8. Ghodki, M.K. An infrared based dust mitigation system operated by the robotic arm for performance improvement of the solar panel. *Sol. Energy* **2022**, *244*, 343–361. [[CrossRef](#)]
9. Yan, Z.; Lai, X.; Meng, Q.; Wu, M. A novel robust control method for motion control of uncertain single-link flexible-joint manipulator. *IEEE Trans. Syst. Man Cybern. Syst.* **2021**, *51*, 1671–1678. [[CrossRef](#)]
10. Benotsmane, R.; Dudás, L.; Kovács, G. Newly elaborated hybrid algorithm for optimization of robot arm's trajectory in order to increase efficiency and provide sustainability in production. *Sustainability* **2021**, *13*, 8193. [[CrossRef](#)]
11. Khosravani, M.R.; Haghghi, A. Large-scale automated additive construction: overview, robotic solutions, sustainability, and future prospect. *Sustainability* **2022**, *14*, 9782. [[CrossRef](#)]
12. Lin, C.J.; Lukodono, R.P. Sustainable human–robot collaboration based on human intention classification. *Sustainability* **2021**, *13*, 5990. [[CrossRef](#)]
13. Parrott, B.; Zanini, P.C.; Shehri, A.; Kotsovos, K.; Gereige, I. Automated, robotic dry-cleaning of solar panels in Thuwal, Saudi Arabia using a silicone rubber brush. *Sol. Energy* **2018**, *171*, 526–533. [[CrossRef](#)]
14. Cammarata, A. Optimized design of a large-workspace 2-DOF parallel robot for solar tracking systems. *Mech. Mach. Theory* **2015**, *83*, 175–186. [[CrossRef](#)]
15. Gregorio, R.D.; Sinatra, R. Singularity curves of a parallel pointing system. *Meccanica* **2002**, *37*, 255–268. [[CrossRef](#)]
16. Kim, J.; Croft, E.A. Full-state tracking control for flexible joint robots with singular perturbation techniques. *IEEE Trans. Control. Syst. Technol.* **2019**, *27*, 63–73. [[CrossRef](#)]
17. Ling, S.; Wang, H.; Liu, P.X. Adaptive fuzzy tracking control of flexible-joint robots based on command filtering. *IEEE Trans. Ind. Electron.* **2020**, *67*, 4046–4055. [[CrossRef](#)]
18. Wei, C.; Xu, J.; Chen, Q.; Song, C.; Qiao, W. Full-order sliding-mode current control of permanent magnet synchronous generator with disturbance rejection. *IEEE J. Emerg. Sel. Top. Ind. Electron.* **2022**. ahead of print. [[CrossRef](#)]
19. Arimoto, S. Learning control theory for robotic motion. *Int. J. Adapt. Control. Signal Process.* **1990**, *4*, 543–564. [[CrossRef](#)]
20. Chi, R.; Hui, Y.; Chien, C.J.; Huang, B.; Hou, Z. Convergence analysis of sampled-data ILC for locally lipschitz continuous nonlinear nonaffine systems with nonrepetitive uncertainties. *IEEE Trans. Autom. Control* **2021**, *66*, 3347–3354. [[CrossRef](#)]
21. Shen, D.; Yu, X. Learning tracking over unknown fading channels based on iterative estimation. *IEEE Trans. Neural Netw. Learn. Syst.* **2022**, *33*, 48–60. [[CrossRef](#)]
22. Jin, X. Nonrepetitive leader-follower formation tracking for multiagent systems with LOS range and angle constraints using iterative learning control. *IEEE Trans. Cybern.* **2019**, *49*, 1748–1758. [[CrossRef](#)] [[PubMed](#)]
23. Chen, Q.; Yu, X.; Sun, M.; Wu, C.; Fu, Z. Adaptive repetitive learning control of PMSM servo systems with bounded nonparametric uncertainties: theory and experiments. *IEEE Trans. Ind. Electron.* **2021**, *68*, 8626–8635. [[CrossRef](#)]
24. Yu, M.; Li, C. Robust adaptive iterative learning control for discrete-time nonlinear systems with time-iteration-varying parameters. *IEEE Trans. Syst. Man Cybern. Syst.* **2017**, *47*, 1737–1745. [[CrossRef](#)]
25. He, W.; Meng, T.; Zhang, S.; Liu, J.K.; Sun, C. Dual-loop adaptive iterative learning control for a timoshenko beam with output constraint and input backlash. *IEEE Trans. Syst. Man Cybern. Syst.* **2019**, *49*, 1027–1038. [[CrossRef](#)]
26. Sun, M.; Zou, S. Adaptive learning control algorithms for infinite-duration tracking. *IEEE Trans. Neural Netw. Learn. Syst.* **2022**. ahead of print. [[CrossRef](#)]
27. Chien, C.J.; Hsu, C.T.; Yao, C.Y. Fuzzy system-based adaptive iterative learning control for nonlinear plants with initial state errors. *IEEE Trans. Fuzzy Syst.* **2004**, *12*, 724–732. [[CrossRef](#)]
28. Sun, M.; Wang, D. Iterative learning control with initial rectifying action. *Automatica* **2002**, *38*, 1177–1182. [[CrossRef](#)]
29. Xu, J.; Xu, J. On iterative learning from different tracking tasks in the presence of time-varying uncertainties. *IEEE Trans. Syst. Man Cybern. Syst.* **2004**, *34*, 589–597. [[CrossRef](#)]
30. Sun, M.; Yan, Q. Error tracking of iterative learning control systems. *Acta Autom. Sin.* **2013**, *39*, 251–262. [[CrossRef](#)]
31. Chen, Q.; Shi, H.; Sun, M. Echo state network-based backstepping adaptive iterative learning control for strict-feedback systems: An error-tracking approach. *IEEE Trans. Cybern.* **2020**, *50*, 3009–3022. [[CrossRef](#)]
32. Sun, M.; Wu, T.; Chen, L.; Zhang, G. Neural AILC for error tracking against arbitrary initial shifts. *IEEE Trans. Neural Netw. Learn. Syst.* **2018**, *29*, 2705–2716. [[CrossRef](#)] [[PubMed](#)]
33. Meng, D.; Zhang, J. Robust tracking of nonrepetitive learning control systems with iteration-dependent references. *IEEE Trans. Syst. Man Cybern. Syst.* **2021**, *51*, 842–852. [[CrossRef](#)]
34. Shen, M.; Wu, X.; Park, J.; Yi, Y.; Sun, Y. Iterative learning control of constrained systems with varying trial lengths under alignment condition. *IEEE Trans. Neural Netw. Learn. Syst.* **2021**. ahead of print. [[CrossRef](#)] [[PubMed](#)]
35. Li, X.; Shen, D.; Xu, J. Adaptive iterative learning control for MIMO nonlinear systems performing iteration-varying tasks. *J. Frankl. Inst.* **2019**, *356*, 9206–9231. [[CrossRef](#)]
36. Huang, J.; Wang, W.; Su, X. Adaptive iterative learning control of multiple autonomous vehicles with a time-varying reference under actuator faults. *IEEE Trans. Neural Netw. Learn. Syst.* **2021**, *32*, 5512–5525. [[CrossRef](#)]
37. Wang, S. Approximation-free control for nonlinear helicopters with unknown dynamics. *IEEE Trans. Circuits Syst. II Express Briefs* **2022**, *69*, 3254–3258. [[CrossRef](#)]
38. Chen, M.; Ge, S.S.; How, B. Robust adaptive neural network control for a class of uncertain mimo nonlinear systems with input nonlinearities. *IEEE Trans. Neural Netw.* **2010**, *21*, 796. [[CrossRef](#)]

39. Xie, S.; Chen, Q.; He, X. Predefined-time approximation-free attitude constraint control of rigid spacecraft. *IEEE Trans. Aerosp. Electron. Syst.* **2022**. *ahead of print*. [[CrossRef](#)]
40. El-Sapa, S.; Lotfy, K.; El-Bary, A. A novel magneto-electron-hole model for optical-thermo-diffusion processes in semiconducting material with variable thermal conductivity. *Silicon* **2022**. *ahead of print*. [[CrossRef](#)]
41. Zhang, C.; Na, J.; Wu, J.; Chen, Q.; Huang, Y. Proportional-integral approximation-free control of robotic systems with unknown dynamics. *IEEE/ASME Trans. Mechatronics* **2022**, *26*, 2226–2236. [[CrossRef](#)]
42. Wang, S.; Yu, H.; Yu, J.; Na, J.; Ren, X. Neural-network-based adaptive funnel control for servo mechanisms with unknown dead-zone. *IEEE Trans. Cybern.* **2020**, *50*, 1383–1394. [[CrossRef](#)] [[PubMed](#)]
43. Li, Y.; Tong, S. Adaptive fuzzy output-feedback stabilization control for a class of switched nonstrict-feedback nonlinear systems. *IEEE Trans. Cybern.* **2017**, *47*, 1007–1016. [[CrossRef](#)] [[PubMed](#)]
44. Tee, K.P.; Ge, S.S.; Tay, E.H. Barrier Lyapunov functions for the control of output-constrained nonlinear systems. *Automatica* **2009**, *45*, 918–927. [[CrossRef](#)]
45. Liu, Y.; Lu, S.; Tong, S.; Chen, X.; Li, D. Adaptive control-based barrier Lyapunov Functions for a class of stochastic nonlinear systems with full state constraints. *Automatica* **2018**, *87*, 83–93. [[CrossRef](#)]
46. Liu, L.; Liu, Y.; Li, D.; Tong, S.; Wang, Z. Barrier Lyapunov function-based adaptive fuzzy FTC for switched systems and its applications to resistance-inductance-capacitance circuit system. *IEEE Trans. Cybern.* **2020**, *50*, 3491–3502. [[CrossRef](#)] [[PubMed](#)]
47. Jin, X. Adaptive fixed-time control for MIMO Nonlinear systems with asymmetric output constraints using universal barrier functions. *IEEE Trans. Autom. Control* **2019**, *64*, 3046–3053. [[CrossRef](#)]
48. He, W.; Yan, Z.; Sun, Y.; Ou, Y.; Sun, C. Neural-learning-based control for a constrained robotic manipulator with flexible joints. *IEEE Trans. Neural Netw. Learn. Syst.* **2018**, *29*, 5993–6003. [[CrossRef](#)] [[PubMed](#)]
49. Sun, W.; Su, S.; Xia, J.; Nguyen, V.T. Adaptive fuzzy tracking control of flexible-joint robots with full-state constraints. *IEEE Trans. Syst. Man Cybern. Syst.* **2019**, *49*, 2201–2209. [[CrossRef](#)]
50. Ma, H.; Zhou, Q.; Li, H.; Lu, R. Adaptive prescribed performance control of a flexible-joint robotic manipulator with dynamic uncertainties. *IEEE Trans. Cybern.* **2021**. *ahead of print*. [[CrossRef](#)]
51. Wang, L.X. *A Course in Fuzzy Systems*; Prentice-Hall: Englewood Cliffs, NJ, USA, 1997.
52. Sun, M. A Barbalat-like lemma with its application to learning control. *IEEE Trans. Autom. Control* **2009**, *54*, 2222–2225. [[CrossRef](#)]